frontiers | Frontiers in Materials

TYPE Original Research
PUBLISHED 01 December 2022
DOI 10.3389/fmats.2022.1037201

OPEN ACCESS

EDITED BY
Safia Akram,
National University of Sciences and Technology, Pakistan

REVIEWED BY
Aurang Zaib,
Federal Urdu University of Arts, Sciences and Technology Islamabad, Pakistan
Emad Aly,
Ain Shams University, Egypt

*CORRESPONDENCE
Zahoor Iqbal,
izahoor@math.qau.edu.pk

SPECIALTY SECTION
This article was submitted to Colloidal Materials and Interfaces, a section of the journal Frontiers in Materials

RECEIVED 05 September 2022
ACCEPTED 04 November 2022
PUBLISHED 01 December 2022

CITATION
Iqbal Z, Yashodha S, Hakeem AKA, Alsawi A, Alyami MA, Yousef ES, Amin AH and Eldin SM (2022), Energy transport analysis in natural convective flow of water:Ethylene glycol (50:50)-based nanofluid around a spinning down-pointing vertical cone. *Front. Mater.* 9:1037201. doi: 10.3389/fmats.2022.1037201

Energy transport analysis in natural convective flow of water: Ethylene glycol (50:50)-based nanofluid around a spinning down-pointing vertical cone

Zahoor Iqbal[1]*, S. Yashodha[2], A. K. Abdul Hakeem[2], Abdulrahman Alsawi[3], Maryam Ahmed Alyami[4], El. Sayed Yousef[5,6], Ali H. Amin[7,8] and Sayed M. Eldin[9]

[1]Department of Mathematics, Quaid-i-Azam University, Islamabad, Pakistan, [2]Department of Mathematics, Sri Ramakrishna Mission Vidyalaya College of Arts and Science, Coimbatore, India, [3]Department of Physics, College of Science, Qassim University, Buraydah, Saudi Arabia, [4]Department of Mathematics, Faculty of Sciences, University of Jeddah, Jeddah, Saudi Arabia, [5]Research Center for Advanced Materials Science (RCAMS), King Khalid University, Abha, Saudi Arabia, [6]Physics Department, Faculty of Science, King Khalid University, Abha, Saudi Arabia, [7]Deanship of Scientific Research, Umm Al-Qura University, Makkah, Saudi Arabia, [8]Zoology Department, Faculty of Science, Mansoura University, Mansoura, Egypt, [9]Faculty of Engineering and Technology, Future University in Egypt, New Cairo, Egypt

The influence of the magnetic field on $H_2O - C_2H_6O_2$ (50:50)-based nanofluid over a heated and spinning vertical cone is deliberated. Water: ethylene glycol (50:50) mixture-based nanofluid with Al_2O_3 and Fe_3O_4 as nanoparticles exhibits higher thermal conductivity enhancement. Heat transfer analysis for the spinning vertical cone with a prescribed surface temperature was investigated. The influence of magnetic parameter, spin parameter, and nanoparticle volume fraction on tangential velocity profile, spin velocity profile, and thermal profile is analyzed. The results accord strongly with the findings of previous research works in the special cases. Computation shows that as magnetic parameter increases, the thicknesses of hydrodynamic and thermal boundary layers decrease and increase, respectively. The addition of nanoparticles (Al_2O_3 and Fe_3O_4) effectively enhances the skin friction coefficient and Nusselt number.

KEYWORDS

spinning down-pointing vertical cone, water–ethylene glycol, nanofluid, transverse magnetic field, heat transport

Introduction

In this industrialized world, the heat transfer process plays a significant role in upgrading the efficiency of industrial applications. To accomplish this global industrialization, in 1995 Choi devised a new progressive class of heat transfer fluids, known as nanofluids (Choi and Eastman, 1995), in which the characteristics of both

nanoparticles and base fluid become efficient. Heat transfer in nanofluid is more proficient than in common fluids. Preparation of nanofluids is not simply the mixture of solids and liquids but requires beneficial methods, as elaborated in Xuan and Li (2000), which presents the procedure for nanofluid preparation. Choosing the nanoparticle and base fluid wisely leads to excellent results depending on the need, as discussed in Usri et al. (2015). Recent research works have been implemented using a novel category of fluids known as nanofluids, which have brought changes widely, including in the industrial, engineering, and medical fields (Vishnu Ganesh et al., 2014; Abdul Hakeem et al., 2017). Different geometrical shapes give different results, including cone and wedge (Anantha Kumar et al. (2018), rotating disk (Gholinia et al. (2019), and vertical cone geometric shapes (CemEce, 2005; Raju and Sandeep, 2016). Nanofluids are the best solutions for heat transfer fluids since they have good thermal performance. Therefore, researchers are proposing suitable models. In this regard, three methods are employed for improving thermal performance (Maleki et al., 2020). To adopt nanofluid applications in daily life, and to increase nanofluid's performance in several applications, nanofluid stability is a critical factor discussed in (Chakraborty and Kumar Panigrahi, 2020). To enhance heat transfer, comparison among different nanofluids for different parameters has been conducted (Dinarvand and Pop, 2017; Aghamajidi et al., 2018). Nanofluid applications have been used in multidisciplinary research. There is a broad range of utilizations in the areas of microalgal cultivation, friction reduction, magnetic sealing, reactor–heat exchange, optical and biomedical applications, nanofluid detergent, electronics cooling, and heating buildings (Vargas-Estrada et al., 2020; Rafiq et al., 2021). With progress in nuclear energy, nanoparticles are also used as coolants in nuclear power plants (Hamidreza Arab BafraniNoori-kalkhoran et al., 2020), in enhancing oil recovery, nano-refrigerants, and nano-lubricants (de Carvalho et al., 2020; SahbanAlnarabiji and Husein, 2020; Salari and Seid Mahdi Jafari, 2020; Mallikarjuna et al., 2021), and in turning and grinding processes (SaswatKhatai et al., 2020). In addition to nanofluid, the flow of hybrid nanofluid across a stretched surface has recently been studied (Aly and Pop, 2019; Aly and Pop, 2020a; Aly and Ebaid, 2020; Aly and Pop, 2020b; Aly et al., 2021; Ahmad et al., 2022; Aly et al., 2022; Arafat et al., 2022; Reddy et al., 2022; Usafzai et al., 2022).

Using a water–ethylene glycol (50:50) combination as the base fluid and Al_2O_3 and Fe_3O_4 as the nanoparticles, we explored the natural convection flow around a heated vertical spinning cone under the influence of a magnetic field.

The aspect of the present work is listed below.

- ➢ Water–ethylene glycol (50:50) mixture is considered a base fluid with Pr = 29.86.
- ➢ Al_2O_3 and Fe_3O_4 are considered to be non-magnetic and magnetic nanoparticles, respectively, which are in thermal equilibrium with base fluid.
- ➢ The geometric cone is used for fluid flow as shown in Figure 1.
- ➢ The effect of viscous dissipation, the resistance heating effect of the fluid, and the slip effect are regarded as negligible.

Governing equations and problem formulation

A continuous two-dimensional flow of a combination of H_2O – $C_2H_6O_2$ (50:50) containing Al_2O_3 and Fe_3O_4 nanoparticles was studied, under the influence of a magnetic field. The flow was laminar, and the nanofluid was assumed to be incompressible.

The y^* axis is the dimension normal to the cone's surface, and the x^* axis is the dimension toward the cone's surface. The rotational angle is indicated by θ, and it was assumed that cone spins with a constant angular velocity Ω.

The models that govern the phenomena are given below (Aghamajidi et al., 2018).

Continuity equation

$$\left(r^*u^*\right)_{x^*} + \left(r^*v^*\right)_{y^*} = 0 \tag{1}$$

TABLE 1 Thermophysical properties of $H_2O - C_2H_6O_2$ (50:50)-based fluid and Al_2O_3/Fe_3O_4 nanoparticles (Aghamajidi et al., 2018; Saranya et al., 2018; Saranya et al., 2022).

	C_p/(J/(kg. K))	ρ/(kg/m^3)	k/(W/(m.K))	$\beta/10^{-5}$(1/K)	σ(Sm^{-1})	Pr
Ethylene glycol and water (50:50) mixture ($H_2O - C_2H_6O_2$) (50:50)	3288	1056	0.425	58	0.00509	29.86
Aluminum oxide (Al_2O_3)	765	3970	40	0.85	35*10^6	—
Magnetite (Fe_3O_4)	670	5180	9.7	1.3	2.5*10^4	—

Momentum equation in *x* direction

$$\rho_{nf}\left((u^{\star})_{x^{\star}}u^{\star} + (u^{\star})_{y^{\star}}v^{\star} - \frac{w^{\star 2}}{x^{\star}}\right) = \mu_{nf}(u^{\star}{}_{y^{\star}})_{y^{\star}} + (\rho\beta)_{nf} g\cos\gamma(T - T_o) - \sigma_{nf}B^2u^{\star} \quad (2)$$

Momentum equation in *y* direction

$$\rho_{nf}\left((w^{\star})_{x^{\star}}u^{\star} + (w^{\star})_{y^{\star}}v^{\star} + \frac{u^{\star}w^{\star}}{x^{\star}}\right) = \mu_{nf}(w^{\star}{}_{y^{\star}})_{y^{\star}} - \sigma_{nf}B^2w^{\star} \quad (3)$$

Energy equation

$$\left(\rho C_p\right)\left(u^{\star}(T)_{x^{\star}} + v^{\star}(T)_{y^{\star}}\right) = k_{nf}\left(T_{y^{\star}}\right)_{y^{\star}} \quad (4)$$

Here, $(r^{\star}u^{\star})_{x^{\star}}$ denotes the partial derivative of $(r^{\star}u^{\star})$ with respect to $x^{\star}$.

The boundary conditions for the above governing equations are given below.

Prescribed surface temperature case:

$$\mathrm{T}(x^{\star},0) = \mathrm{T}_0 + (\mathrm{T_r}{-}\mathrm{T}_0)\frac{x^{\star}}{L} \text{ when } y^{\star} = 0 \quad (5)$$

$$u^{\star} = 0,\ v^{\star} = 0,\ w^{\star} = r^{\star}\Omega \text{ as } \mathrm{y}^{\star} = 0 \quad (6)$$

$$u^{\star} \to 0,\ w^{\star} \to 0, \mathrm{T} \to 0 \text{ as } y^{\star} \to \infty\ . \quad (7)$$

γ is considered as half of the vertex angle, and the local radius of the cone is considered as $\mathrm{r} = x\sin\gamma$. Dimensional velocity components are denoted by $u^{\star}$, $v^{\star}$, and $w^{\star}$ in the $x^{\star}$, $y^{\star}$, and θ directions, respectively.

The thermophysical properties are given in Table 1. The nanofluid properties are given by (Saranya et al., 2022)

$$\text{Nanofluid's kinematic viscosity, } \nu_{nf} = \frac{\mu_f}{(1-\phi)^{2.5}\left[(1-\phi)\rho_f + \phi\rho_s\right]} \quad (8)$$

$$\text{Nanofluid's density } \rho_{nf} = (1-\phi)\rho_f + \phi\rho_s \quad (9)$$

$$\text{Nanofluid's thermal diffusivity, } \alpha_{nf} = \frac{k_{nf}}{(\rho C_p)_{nf}}\ , \quad (10)$$

$$\text{Nanofluid's heat capacitance, } (\rho C_p)_{nf} = (1-\phi)(\rho C_p)_f + \phi(\rho C_p)_s, \quad (11)$$

$$\text{Coefficient of thermal expansion, } (\rho\beta)_{nf} = (1-\phi)(\rho\beta)_f + \phi(\rho\beta)_s \quad (12)$$

Nanofluid's thermal conductivity and electrical conductivity are given by

$$\frac{k_{nf}}{k_f} = \frac{\left(k_s + 2k_f\right) - 2\phi\left(k_f - ks\right)}{\left(k_s + 2k_f\right) + \phi\left(k_f - ks\right)} \text{ and } \frac{\sigma_{nf}}{\sigma_f} = 1 + \frac{3(\sigma-1)\phi}{(\sigma+2) - (\sigma-1)\phi}, \text{ where} \sigma = \frac{\sigma_s}{\sigma_f}, \text{ respectively} \quad (13)$$

Here, ϕ is the solid volume fraction. The subscripts sf, nf, and s denote the fluid, nanofluid, and solid, respectively.

For the current analysis, the following variables are utilized (Aghamajidi et al., 2018):

$$r = \frac{r^{\star}}{L},\ x = \frac{x^{\star}}{L},\ y = \frac{y^{\star}}{L}Gr^{1/4} \quad (14)$$

$$u = \frac{u^{\star}}{U}\ ,\ v = \frac{v^{\star}}{U}Gr^{1/4},\quad w = \frac{w^{\star}}{\Omega L}\ ,\ \Theta = \frac{T - T_0}{T_r - T_0} \quad (15)$$

where u, v, and w represent the velocity components x direction, y direction, and θ direction, respectively, and Θ is the dimensionless temperature ratio. $r = x\sin\gamma$ is the radius of the cone and the magnetic field strength is $\mathrm{B} = B_0\,\mathrm{b}(\mathrm{x})/(r\sqrt{1-r'^2})$.

The Prandtl number (Pr), reference velocity (U), and Grashof number (Gr) are defined as

$$Pr = \frac{\nu}{\alpha},\ U = \left[\mathrm{g}\cos\gamma\beta L(T_r - T_0)\right]^{1/2},\ Gr = \left(\frac{UL}{\nu}\right)^2 \quad (16)$$

where β is the thermal expansion coefficient, L is the reference length, ν is kinematic viscosity, and α is thermal diffusivity. T_r is any taken reference temperature unequal to the ambient temperature T_0.

The governing equations from Eq. 1 to Eq. 4 take the following non-dimensional form after substituting the dimensionless variables, as defined in Eqs 14–16:

$$(ru)_x + (rv)_y = 0 \quad (17)$$

$$uu_x + vu_y - \frac{Re^2}{Gr}\frac{r'}{r}w^2 = \frac{1}{\left[(1-\phi) + \phi\left(\rho_s/\rho_f\right)\right]}\left\{\frac{1}{(1-\phi)^{2.5}}\left(u_y\right)_y + \left[(1-\phi) + \phi(\rho\beta)_s/(\rho\beta)_f\right]\Theta - \frac{\sigma_{nf}}{\sigma_f}M\Lambda^2u\right\} \quad (18)$$

$$uw_x + vw_y + uw\frac{r'}{r} = \frac{1}{\left(1 - \phi + \phi\rho_s/\rho_f\right)}\left\{\frac{1}{(1-\phi)^{2.5}}\left(w_y\right)_y - \left(\frac{\sigma_{nf}}{\sigma_f}\right)M\Lambda^2w\right\} \quad (19)$$

$$u\Theta_x + v\Theta_y = \frac{1}{\left[(1-\phi) + \phi\left((\rho C_p)_s/(\rho C_p)_f\right)\right]}\left[\left(\frac{1}{Pr}\frac{K_{nf}}{K_f}\right)\left(\Theta_y\right)_y\right] \quad (20)$$

The boundary conditions are given below.

Prescribed surface temperature case:

$$\Theta = x \text{ as } \mathrm{y} = 0 \quad (21)$$

$$u = 0,\ v = 0,\ w = r \text{ as } \mathrm{y} = 0 \quad (22)$$

$$\mathrm{u} \to 0,\ \mathrm{w} \to 0,\ \Theta \to 0 \quad \text{as} \quad y \to \infty \quad (23)$$

The rotational Reynolds number, the magnetic field function Λ, and the magnetic parameter are

TABLE 2 Comparison with the results of Ece (2006), Dinarvand (2011), and Aghamajidi et al. (2018) for regular fluid ($\phi = 0$), for the effect of M and ϵ on $F^{II}(0)$ and $-H^{I}(0)$ with prescribed surface temperature, for Prandtl number =1.

ϵ	M	$F^{II}(0)$				$-H^{I}(0)$			
		Ece (2006)	Dinarvand (2011)	Aghamajidi et al. (2018)	Present results	Ece (2006)	Dinarvand (2011)	Aghamajidi et al. (2018)	Present results
0.0	**0.0**	0.68150	0.68151	0.68151	0.681483	0.63887	0.63887	0.63887	0.638854
	1.0	0.55976	0.55975	0.55976	0.559761	0.55869	0.55867	0.55868	0.558692
	2.0	0.48679	0.48675	0.48678	0.486807	0.50338	0.50341	0.50339	0.503352
0.5	**0.0**	0.84651	0.84654	0.84651	0.846488	0.67194	0.67196	0.67194	0.671938
	1.0	0.68548	0.68553	0.68549	0.685480	0.58138	0.58142	0.58137	0.581380
	2.0	0.59003	0.59010	0.59003	0.590045	0.51968	0.51963	0.51969	0.519638
1.0	**0.0**	1.00196	1.00191	1.00195	1.001943	0.70053	0.70056	0.70053	0.700524
	1.0	0.80819	0.80826	0.80820	0.808193	0.60256	0.60250	0.60257	0.602564
	2.0	0.69204	0.69203	0.69205	0.692051	0.53536	0.53543	0.53535	0.535337

$$Re = \frac{\Omega L^2}{\nu_f},\ \Lambda = \frac{b(x)}{r\sqrt{1-r'^2}}, M = \frac{\sigma_f B_0^2 L}{U\rho_f}. \tag{24}$$

The function $b(x) = r\sqrt{1-r'^2}$ is the basis of the current analysis, which was conducted in a scenario in which the intensity of the magnetic field applied normal to the surface was uniform along the surface within the boundary layer, such that $\Lambda = 1$:

$$ru = \psi_y \quad , rv = -\psi_x\,, \tag{25}$$

where ψ is stream function and the boundary layer variables can be presented as

$$\psi(x,y) = xrF(y),\ w = rG(y),\ \Theta = xH(y), \tag{26}$$

Applying the boundary layer variables as written in Eq. 26, the non-dimensional governing Eqs 17–20 are converted into the system of Ordinary differential equations (ODEs).

Here F(y), G(y), and H(y) represent the tangential velocity profile, swirl velocity profile, and temperature profile, respectively.

$$A_1F''' + 2FF'' - F'^2 + \varepsilon G^2 - A_2A_5M\Lambda^2F' + A_3H = 0 \tag{27}$$

$$A_1G'' + 2FG' - 2GF' - A_2A_5M\Lambda^2G = 0 \tag{28}$$

$$A_4H'' + \Pr\left[2FH' - F'H\right] = 0 \tag{29}$$

where $A_1 = 1/(1-\phi)^{2.5}(1-\phi+\phi(\rho_s/\rho_f))$, $A_2 = 1/(1-\phi+\phi(\rho_s/\rho_f))A_3 = (1-\phi+\phi(\rho\beta)_s/(\rho\beta)_f)/(1-\phi+\phi(\rho_s/\rho_f))$, $A_4 = (k_{nf}/k_f)/(1-\phi+\phi(\rho C_p)_s/(\rho C_p)_f)A_5 = \sigma_{nf}/\sigma_f = 1+3(\sigma-1)\phi/(\sigma+2)-(\sigma-1)\phi$, where $\sigma = \sigma_s/\sigma_f\varepsilon = (\mathrm{Resin}\gamma)^2/\mathrm{Gr}$ is the spin parameter.

The boundary conditions from Eqs 21 to 23 are reduced to

$$F = 0,\ F' = 0, G = 1, H = 1\ as\ y = 0 \tag{30}$$

$$F' \to 0,\ G \to 0,\ H \to 0\ as\ y \to \infty \tag{31}$$

Skin friction coefficient and local Nusselt number

The skin friction coefficient C_f and the local Nusselt number (Nu), have been consequential in the engineering field and are defined as

$$C_f = \frac{2\tau_w}{\rho_f U^2},\ \mathrm{Nu} = \frac{Lq_w}{k_f(T_w - T_\infty)} \tag{32}$$

where τ_w is the skin friction and q_w is the surface heat flux, written as

$$\tau_w = \mu_{nf}\left(\frac{\partial u^*}{\partial y^*}\right)_{y^*=0}, q_w = -k_{nf}\left(\frac{\partial T}{\partial y^*}\right)_{y^*=0} \tag{33}$$

Using the non-dimensional transformations, we obtain

$$C_f\mathrm{Gr}^{1/4} = 2\left(\frac{\mu_{nf}}{\mu_f}\right)xF''(0), \mathrm{NuGr}^{-1/4} = -\left(\frac{k_{nf}}{k_f}\right)xH'(0) \tag{34}$$

Numerical approach

Eqs 27–29 with boundary conditions (Eqs 30, 31) specify nonlinear ordinary differential equations. By using a fourth-order Runge–Kutta finite difference scheme and shooting approach, this model is solved numerically to examine the effects of M, ϵ, ϕ on $F^I(y)$, G(y), H(y), C_f, and Nu.

We represent $F = y_1$, $G = y_4$, $H = y_6$ for our present problem and the important steps of the method as

$$y_1' = y_2$$
$$y_2' = y_3$$
$$y_3' = -1/A_1\left[2y_1y_3 - y_2^2 + \varepsilon y_4^2 - A_2A_5M\Lambda^2y_2 + A_3y_6\right]$$
$$y_4' = y_5$$

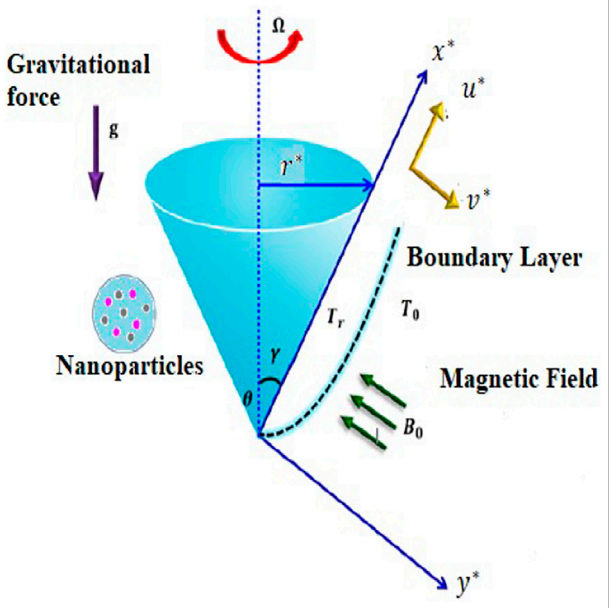

FIGURE 1
Geometry of the problem.

$$y_5' = -1/A_1\left[\left(2y_1y_5 - 2y_2y_4\right) - A_2A_5M\Lambda^2y_4\right]$$
$$y_6' = y_7$$
$$y_7' = -1/A_4\left[\Pr\left(2y_1y_7 - y_2y_6\right)\right]$$

To authenticate our work, the outcomes were compared with the results of Ece (2006), Dinarvand (2011), and Aghamajidi et al. (2018), which are shown in Table 2. It is worth mentioning that the present outcomes have excellent compatibility with the solutions obtained by Ece (2006), Dinarvand (2011), and Aghamajidi et al. (2018) for the case $\phi = 0$.

Results and discussion

The effects of spin parameter ϵ, nanoparticle volume fraction ϕ, and magnetic parameter M on tangential velocity profile $F^l(y)$, swirl velocity profile G(y), and temperature profile H(y) for the case of prescribed surface temperature were plotted.

The tangential velocity profile decreases as the range of magnetic parameters increases. This is because a magnetic field creates a drag force, known as the Lorentz force, in an electrically conducting fluid. There is a dip in the velocity profile due to this significant resistive force acting counter to the direction of fluid flow. As a result, as M becomes stronger, the hydrodynamic boundary layer thickness becomes thinner. Fe_3O_4 has higher tangential velocity than Al_2O_3. In the case of swirl velocity, as the magnetic parameter increases, swirl velocity decreases. Al_2O_3 has higher swirl velocity than Fe_3O_4, as described in Figure 2

Boundary layer behaviour for the case of prescribed surface temperature

To overcome drag force, the fluid must do some additional work, which is transformed into thermal energy and leads to an increase in the temperature of the fluid. Al_2O_3

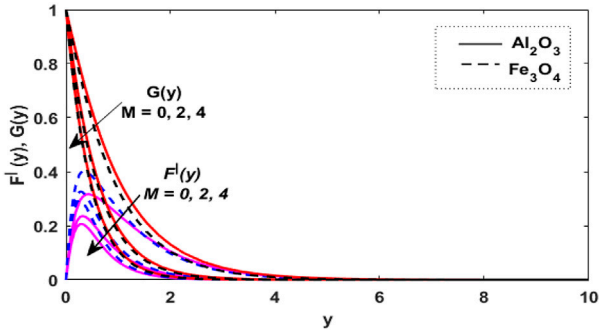

FIGURE 2
Influence of M on $F^l(y)$ and G(y) when $\phi = 0.01$, $\epsilon = 1$, and Pr = 29.86.

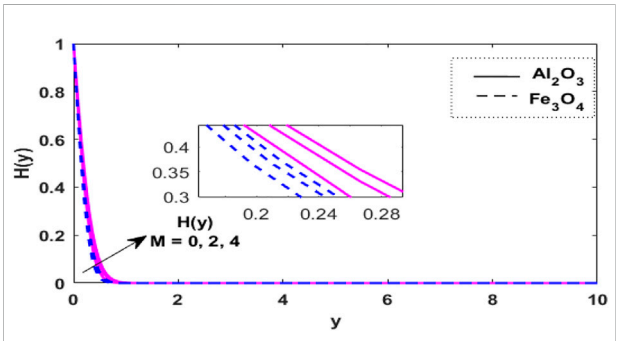

FIGURE 3
Influence of M on H(y) when $\phi = 0.01$, $\epsilon = 1$, and Pr = 29.86.

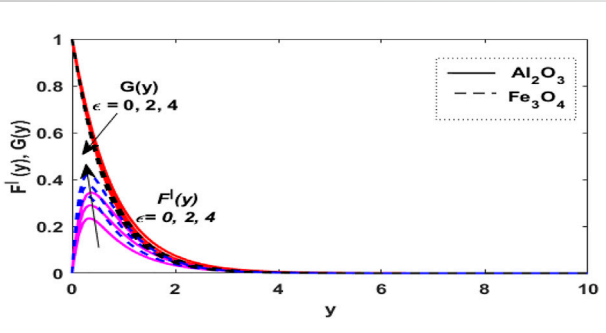

FIGURE 4
Characteristics of ϵ on $F^l(y)$ and G(y), when $\phi = 0.01$, M = 1, and Pr = 29.86.

has a higher temperature than Fe_3O_4. Therefore, as the strength of M increases, the thickness of the thermal boundary value rises, as described in Figure 3. From the physical point of view, as the nanoparticles transfer or dissipate heat, they cause a larger thermal boundary layer thickness and, finally, the intensification in the temperature of the fluid.

As the spin parameter appears in the momentum equation, the effect of spin parameter is more in this equation, and increased values of the spin parameter dynamically promote tangential velocity. Fe_3O_4 has higher tangential velocity than Al_2O_3. Swirl velocity drops as spin parameter increases near the surface of the cone, as shown in Figure 4.

Temperature is reduced as spin parameter increases. Therefore, there is reduction in the thickness of the thermal boundary layer for varying magnitudes of spin parameter. Fe_3O_4 nanoparticles are compressed more toward the surface than are the Al_2O_3 nanoparticles as the spin parameter rises, as indicated in Figure 5.

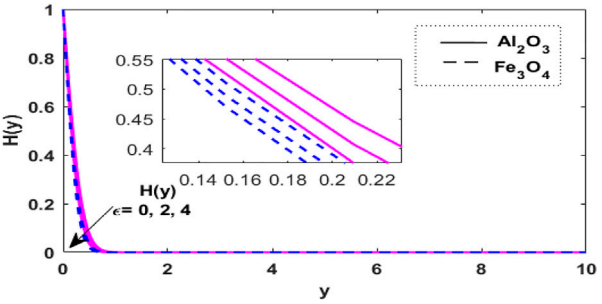

FIGURE 5
Impact of ϵ on H(y), when ϕ = 0.01, M = 1, and Pr = 29.86.

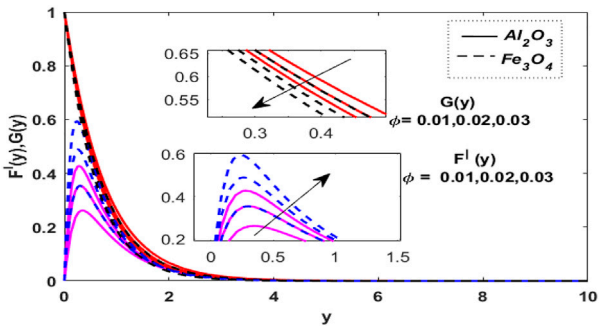

FIGURE 6
Variation of φ on F'(y) and G(y) when ϵ = 1, M = 1, and Pr = 29.86.

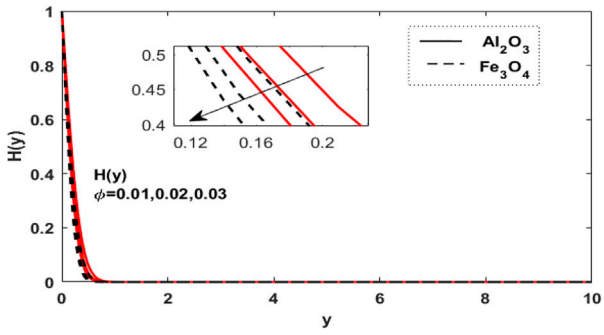

FIGURE 7
Variation of ϕ on H(y) when ϵ = 1, M = 1, and Pr = 29.86.

The influence of nanoparticle volume fraction on tangential and swirl velocity profile is depicted in Figure 6. As the value of ϕ rises, the tangential velocity of the flow increases. The opposite behavior is examined in the case of swirl velocity profile.

In Figure 7, the influence of the Al_2O_3 and Fe_3O_4 nanoparticle volume fraction for thermal distribution is plotted. Analysis of this plot showed that the temperature distribution builds up by enhancing the volume fraction of Al_2O_3.

The coefficient of skin friction and Nusselt number

Table 3 shows the variation of skin friction coefficient and nusselt number for different values of solid volume fraction, spin parameter and magnetic parameter. It is found that

TABLE 3 The coefficient of skin friction and Nusselt number.

φ	ε	M	Pr	(1/x) $C_fGr^{(1/4)}$		(1/x) $NuGr^{-1/4}$	
				Al_2O_3	Fe_3O_4	Al_2O_3	Fe_3O_4
0.01	1	1	29.86	4.1880	6.5685	3.1603	3.6685
0.02				6.6672	10.7914	3.7276	4.3681
0.03				8.9413	14.6327	4.1515	4.8770
0.04				11.1076	18.2739	4.5059	5.2963
0.01	1.0	1	29.86	4.1879	6.5685	3.1603	3.6685
	2.0			3.9995	6.3515	3.0638	3.5858
	3.0			3.8639	6.1865	2.9920	3.5216
	4.0			3.7556	6.0507	2.9334	3.4677
0.01	1	1.0	29.86	4.1879	6.5684	3.1603	3.6685
		2.0		4.5756	6.9253	3.2806	3.7542
		3.0		4.9609	7.2799	3.3921	3.8353
		4.0		5.3430	7.6321	3.4958	3.9125

magnetic nanoparticles have high skin friction and nusselt number values.

Conclusion

The numerical solution was achieved using the fourth-order Runge–Kutta method combined with boundary conditions and shooting methods to the non-dimensional ODEs. The following graph-related points are noteworthy:

- ➢ Intensification of the extent of spin parameter dynamically promotes the tangential velocity, and Fe_3O_4 has a higher tangential velocity than Al_2O_3.
- ➢ Higher magnetic parameters decrease the momentum transport of hydrodynamic flow and accelerate thermal transport in the presence of $H_2O - C_2H_6O_2$ (50:50) mixture.
- ➢ Higher spin parameter reduces the thermal profile of nanofluid.
- ➢ The tangential velocity of Fe_3O_4 is shown to be greater than for the Al_2O_3 nanoparticle.
- ➢ It is worth mentioning that the present outcomes are highly compatible with solutions obtained in previous research for the special case.

Data availability statement

The original contributions presented in the study are included in the article/supplementary material; further inquiries can be directed to the corresponding author.

Author contributions

All authors listed have made a substantial, direct, and intellectual contribution to the work and approved it for publication.

Acknowledgments

The authors express their appreciation to "The Research Center for Advanced Materials Science (RCAMS)" at King Khalid University, Saudi Arabia, for funding this work under the grant number RCAMS/KKU/002-22. The authors would like to thank the Deanship of Scientific Research at Umm Al-Qura University for supporting this work by Grant Code (22UQU4331100DSR18).

Conflict of interest

The authors declare that the research was conducted in the absence of any commercial or financial relationships that could be construed as a potential conflict of interest.

Publisher's note

All claims expressed in this article are solely those of the authors and do not necessarily represent those of their affiliated organizations, or those of the publisher, the editors, and the reviewers. Any product that may be evaluated in this article, or claim that may be made by its manufacturer, is not guaranteed or endorsed by the publisher.

References

Abdul Hakeem, A. K., Saranya, S., and Ganga, B. (2017). Comparative study on Newtonian/non-Newtonian base fluids with magnetic/non-magnetic nanoparticles over a flat plate with uniform heat flux. *J. Mol. Liq.* 230, 445–452. doi:10.1016/j.molliq.2016.12.087

Aghamajidi, Mohammad, EftekhariYazdi, Mohammad, Dinarvand, Saeed, and Pop, Ioan (2018). Tiwari-Das nanofluid model for magnetohydrodynamics (MHD) naturalconvective flow of a nanofluid adjacent to a spinning down-pointing vertical cone. *Propuls. Power Res.* 7 (1), 78–90. doi:10.1016/j.jppr.2018.02.002

Ahmad, N. P., Indumathi, N., Ganga, B., Charles, S., Hakeem, A. K. A., Iqbal, Z., et al. (2022). Forced convection of non-Darcy flow of ethylene glycol conveying copper (II) oxide and titanium dioxide nanoparticles subject to lorentz force on wedges: Non-Newtonian Casson model. *Front. Chem.* 10, 1010591. doi:10.3389/fchem.2022.1010591

Aly, E. H., and Ebaid, A. (2020). MHD Marangoni boundary layerproblem for hybrid nanofluidswith thermal radiation. *Int. J. Num. Meth. Heat Fluid Flow*.31.

Aly, E. H., Mahabaleshwar, U. S., Anusha, T., Usafzai, W. K., and Pop, I. (2022). Wall jet flow and heat transfer of a hybrid nanofluid subject to suction/injection with thermal radiation. *Therm. Sci. Eng. Prog.* 32 (1), 101294. doi:10.1016/j.tsep.2022.101294

Aly, E. H., and Pop, I. (2020). Merkin and Needham wall jet problem for hybrid nanofluids withthermal energy. *Eur. J. Mech. - B/Fluids* 83, 195–204. doi:10.1016/j.euromechflu.2020.05.004

Aly, E. H., and Pop, I. (2020). MHD flow and heat transfer near stagnation point over a stretching/shrinking surface with partial slip and viscous dissipation: Hybrid nanofluid versus nanofluid. *Powder Technol.* 367, 192–205. doi:10.1016/j.powtec.2020.03.030

Aly, E. H., and Pop, I. (2019). MHD flow and heat transfer over a permeable stretching/shrinking sheet in a hybrid nanofluid with a convective boundary condition. *Int. J. Numer. Methods Heat. Fluid Flow.* 29 (9), 3012–3038. doi:10.1108/hff-12-2018-0794

Aly, E. H., Rosca, A. V., Rosca, N. C., and Pop, I. (2021). Convective heat transfer of a hybrid nanofluid over a nonlinearly stretching surface with radiation effect. *Mathematics* 9, 2220. doi:10.3390/math9182220

Anantha Kumar, K., Ramana Reddy, J. V., Sugunamma, V., and Sandeep, N. (2018). Magnetohydrodynamic Cattaneo-Christov flow past a cone and a wedge with variable heat source/sink. *Alexandria Eng. J.* 57, 435–443. doi:10.1016/j.aej.2016.11.013

Arafat, H., Iqbal, Z., T-Eldin, E., Almohiemn, M., Yassin, M. F., Guedri, K., et al. (2022). Energy transport features of Oldroyd-B nanofluid flow over bidirectional stretching surface subject to Cattaneo-Christov heat and mass fluxes. *Front. Energy Res.* 10, 1361. doi:10.3389/fenrg.2022.985146

CemEce, Mehmet (2005). Free convection flow about a cone under mixed thermal boundary conditions and a magnetic field. *Appl. Math. Model.* 29, 1121–1134. doi:10.1016/j.apm.2005.02.009

Chakraborty, Samarshi, and Kumar Panigrahi, Pradipta (2020). Stability of nanofluid: A review. *Appl. Therm. Eng.* 174, 115259. doi:10.1016/j.applthermaleng.2020.115259

Choi, S. U. S., and Eastman, J. A. (1995). *Enhancing thermal conductivity of fluids with nanoparticles*. ASME International Mechanical Engineering Congress & Exposition, San Francisco, CA, November 12–17, 1995.

De Carvalho, J. E. S. P., Sotomayor, P. O., Parise, J. A. R., and Florian, P. (2020). Numerical assessment of critical properties of nanofluids: Applications to nanorefrigerants and nanolubricants. Journal of Molecular Liquids, 318, doi:10.1016/j.molliq.2020.113938

Dinarvand, Saeed, and Pop, Ioan (2017). Free-convective flow of copper/water nanofluid about a rotating down-pointing cone using Tiwari-Das nanofluid scheme. *Advanced Powder Technology*, 28, doi:10.1016/j.apt.2016.12.016

Dinarvand, S. (2011). The laminar free-convection boundary-layer flow about a heated and rotating down-pointing vertical cone in the presence of a transverse magnetic field. *Int. J. Numer. Meth. Fluids* 67 (12), 2141–2156. doi:10.1002/fld.2489

Ece, M. C. (2006). Free convection flow about a vertical spinning cone under a magnetic field. *Appl. Math. Comput.* 179, 231–242. doi:10.1016/j.amc.2005.11.099

Gholinia, M., Hosseinzadeh, Kh., Mehrzadi, H., Ganji, D. D., and Ranjbar, A. A. (2019). Investigation of MHD Eyring–Powell fluid flow over a rotating disk under effect of homogeneous–heterogeneous reactions. *Case Stud. Therm. Eng.* 13, 100356. doi:10.1016/j.csite.2018.11.007

Hamidreza, A. B., Omid, N.-K., Massimiliano, G., Rohollah, A., and Mohammad, M. M. (2020). On the use of boundary conditions and thermophysical properties of nanoparticles for application of nanofluids as coolant in nuclear power plants; a numerical study. *Prog. Nucl. Energy* 126, 103417. doi:10.1016/j.pnucene.2020.103417

Maleki, Akbar, Elahi, Milad, Mamdouh El Haj AssadAlhuyi Nazari, Mohammad, Mostafa Safdari Shadlooand Nabipour, Narjes (2020). Thermal conductivity modeling of nanofluids with ZnO particles by using approaches based on artificial neural network and MARS. *J. Therm. Anal. Calorim.* 143, 4261–4272. doi:10.1007/s10973-020-09373-9

Mallikarjuna, K., Santhoshkumar Reddy, Y., Hemachandra Reddy, K., and Sanjeeva Kumar, P. V. (2021). A nanofluids and nanocoatings used for solar energy harvesting and heat transfer applications: A retrospective review analysis. *Mater. Today Proc.* 37, 823–834. doi:10.1016/j.matpr.2020.05.833

Rafiq, Muhammad, Shafique, Muhammad, Azam, Anam, and Ateeq, Muhammad (2021). Transformer oil-based nanofluid: The application of nanomaterials on thermal, electrical and physicochemical properties of liquid insulation-A review. *Ain Shams Eng. J.* 12, 555–576. doi:10.1016/j.asej.2020.08.010

Raju, C. S. K., and Sandeep, N. (2016). Heat and mass transfer in MHD non-Newtonian bio-convection flow over a rotating cone/plate with cross diffusion. *J. Mol. Liq.* 215, 115–126. doi:10.1016/j.molliq.2015.12.058

Reddy, S. C., Asogwa, K. K., Yassen, M. F., AdnanIqbal, Z., M-Eldin, S., et al. (2022). Dynamics of MHD second-grade nanofluid flow with activation energy across a curved stretching surface. *Front. Energy Res.* 10, 1007159. doi:10.3389/fenrg.2022.1007159

SahbanAlnarabiji, Mohamad, and Husein, Maen M. (2020). Application of bare nanoparticle-based nanofluids in enhanced oil recovery. *Fuel* 267, 117262. doi:10.1016/j.fuel.2020.117262

Salari, Saeed, and Seid Mahdi Jafari (2020). Application of nanofluids for thermal processing of food products. *Trends Food Sci. Technol.* 97, 100–113. doi:10.1016/j.tifs.2020.01.004

Saranya, Shekar, Baranyi, László, and Qasem, M. (2022). Al- Free convection flow of hybrid ferrofluid past a heated spinning cone. *Therm. Sci. Eng. Prog.*

Saranya, S. Ragupathi, P. Ganga, B., Sharma, R. P. and Abdul Hakeem, A. K. (2018). Non-linear radiation effects on magnetic/non-magnetic nanoparticles with different base fluids over a flat plate. *Advanced Powder Technology*, 29, doi:10.1016/j.apt.2018.05.002

SaswatKhatai, Ramanuj Kumar, Ashok Kumar Sahoo, Panda, Amlana, and Das, Diptikanta (2020). Metal-oxide based nanofluid application in turning and grinding processes: A comprehensive review. *Mater. Today Proc*.

Usafzai, W. K., Aly, E. H., Alshomrani, A. S., and Ullah, M. Z. (2022). Multiple solutions for nanofluids flow and heat transfer in porous medium with velocity slip and temperature jump. *Int. Commun. Heat Mass Transf.* 131, 105831. doi:10.1016/j.icheatmasstransfer.2021.105831

Usri, N. A., Azmi, W. H., Rizalman, M., Abdul Hamid, K., and Najafi, G. (2015). Thermal conductivity enhancement of Al_2O_3 nanofluid in ethylene glycol and water mixture, 2015 international conference on alternative energy in developing countries and emerging economies. *Energy Procedia* 79, 397–402. doi:10.1016/j.egypro.2015.11.509

Vargas-Estrada, Laura, Torres-Arellano, S., Longoria, Adriana, Dulce, M., Arias, Patrick U., and Sebastian, P. J. (2020). Role of nanoparticles on microalgal cultivation: A review. *Fuel* 280, 118598. doi:10.1016/j.fuel.2020.118598

Vishnu Ganesh, N., Ganga, B., and Abdul Hakeem, A. K. (2014). Lie symmetry group analysis of magnetic field effects on free convective flow of a nanofluid over a semi-infinite stretching sheet. *J. Egypt. Math. Soc.* 22, 304–310. doi:10.1016/j.joems.2013.08.003

Xuan, Yimin, and Li, Qiang (2000). *Heat transfer enhancement of nanofluids, school of power EngineeringP*. Nanjing: Nanjing University of Science and Technology. eople's Republic of China.

Nomenclature

k thermal conductivity, $Wm^{-1}K^{-1}$

H dimensionless fluid temperature

G dimensionless swirl velocity

$\mathbf{C_p}$ specific heat, $Jkg^{-1}K^{-1}$

M magnetic parameter

F dimensionless tangential velocity

g acceleration due to gravity, ms^{-2}

L reference length, m

$\mathbf{Nu_x}$ local Nusselt number

$\mathbf{C_f}$ skin friction coefficient

B magnetic field intensity, $kgs^{-2}A^{-1}$

$\mathbf{q_w}$ surface heat flux, Wm^{-2}

r dimensionless radius

$\mathbf{T_r}$ reference temperature, K

Gr Grashof number

$\mathbf{T_o}$ temperature of the cone surface, K

Pr Prandtl number

u,v,w velocity component in the x,y,z direction respectively

T temperature, K

Re local Reynolds number

y dimensionless coordinate normal to the surface

U reference velocity, ms^{-1}

x dimensionless coordinate measured along the surface

β thermal expansion coefficient, K^{-1}

ϕ nanoparticle volume fraction

ε spin parameter

τ_w skin friction, Nm^{-2}

γ half of vertex angle

ρ density, kgm^{-3}

ψ dimensionless stream function

Ω angular velocity of the cone

θ angle of rotation

υ kinematic viscosity, m^2s^{-1}

Θ dimensionless temperature ratio

σ electrical conductivity, Sm^{-1}

α thermal diffusivity, m^2s^{-1}

μ dynamic viscosity, $kgm^{-1}s^{-1}$